23rd ABCM International Congress of Mechanical Engineering
December 6-11, 2015, Rio de Janeiro, RJ, Brazil

MONITORING FUNCTION BASED EXTREMUM SEEKING FOR FUEL CELL ENERGY APPLICATIONS

Tiago Roux Oliveira
Téo Cerqueira Revoredo
Dept. of Electronics and Telecommunication Engineering, State University of Rio de Janeiro (UERJ), RJ 20550-900, Brazil.
Emails: tiagoroux@uerj.br, teorevoredo@uerj.br

Abstract. *The principles of Extremum Seeking (ES) were invented in the last century and it is one of the oldest feedback control methods. Rather than regulation, its purpose is real-time optimization. For this reason, applications of ES have often come from energy systems. In the ensuing decades, ES has been applied to gas turbines and even nuclear fusion reactors. Renewable energy applications have brought a new focus on the capabilities of ES algorithms, such as wind and solar energy. In this article, we present applications of ES in a different type of energy conversion systems for renewable energy sources: fuel cell systems. We introduce a new ES algorithm based on monitoring functions to control the current input of a fuel cell system subject to a constant air flow into the cathode. The method does not rely on knowledge of system modeling parameters, and adapt to changes in those parameters that occur due to disturbances or degradation. In a nutshell, the goal is the extraction of the maximum feasible energy from the system under uncertainty and in the absence of a priori modeling knowledge about the fuel cell system. The convergence rate of such a design to the maximum power point tracking is independent of the plant parameters, with tunable transient performance which is also independent of environmental conditions. We present simulation results that show the effectiveness of the proposed controller in comparison with the existing ES approaches.*

Keywords: *maximum power point tracking, extremum seeking, monitoring functions, renewable energy, fuel cell systems.*

1. INTRODUCTION

Electricity is one of the main pillars of modern society's evolution and the need to ensure the sustainability of power generation is of great importance. Hence, research and development for the improvement of alternative forms of power generation gains importance in energy systems. One alternative for a good sort of application is the use of fuel cells (FC), which are electrochemical devices that convert the chemical energy of a reaction into electrical energy (U.S. Department of Energy, 2000), as illustrated in Figure 1. They can be used as a power generation alternative in many applications ranging from portable electronics charging to buildings power plants, including automobiles use. In our study, the Proton Exchange Membrane Fuel Cell (PEMFC) is considered.

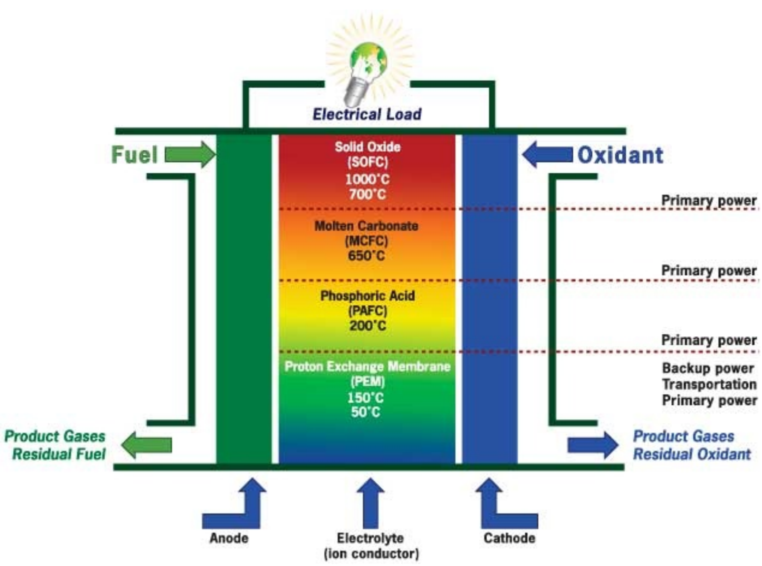

Figure 1. General scheme of a fuell cell (CaSFCC, 2015).

Fuel cell research played a secondary role in the power generation until not long ago, due to the cost of the materials involved and the need for a certain amount of storage energy to allow its operation. On the other hand, one can mention some advantages such as low pollutants emission and the capability a fuel cell system possesses of renewing fuel. In addition, a fuel cell stack is modular and therefore provides the possibility to be built for a wide range of electrical power systems, ranging from mili to mega Watts. Based on such advantages, this work hereby presents a way to reduce costs through increased efficiency operation of a fuel cell through the use of Extremum Seeking Control algorithms.

Extremum Seeking Control (Krstić, 2014), or simply Extremum Seeking (ES), is based on the use of dither perturbation and adaptation to achieve desired control inputs. The biggest advantage of this method is that it is able to improve the system performance even without the complete knowledge of its model. In this sense, we apply ES to perform an online search for maximum or minimum points of a given process (Yau and Wu, 2011).

In this paper, two different ES control approaches for fuel cell systems are discussed, one is based on sinusoidal dither disturbance (Krstić, 2014) and the proposed one, which uses switching monitoring function (Aminde *et al.*, 2013). Numerical simulations show that both methods present promising results.

2. MATHEMATICAL MODEL OF THE FUEL CELL

The mathematical models of a fuel cell used in the literature differs in complexity in accordance to the purpose of the fuel cell system discussed. Here, the aim is to study the response of a FC due to an electric current input control. The mathematical equations are presented below.

The output voltage of a fuel cell can be defined as in (Revoredo, 2011):

$$V_{FC} = E_{Nerst} - V_{act} - V_{Ohmic} - V_{con} \,, \tag{1}$$

where E_{Nerst} is the thermodynamic potential of the cell (open circuit voltage), V_{Act} is the loss due to the activation of the anode and cathode, V_{ohmic} is the ohmic loss and V_{con} is the loss due to mass transport, which will be better detailed later on. Figure 2 illustrates the voltage response of a cell V_{FC} including the voltage potential losses to an electric current input, I_{FC}.

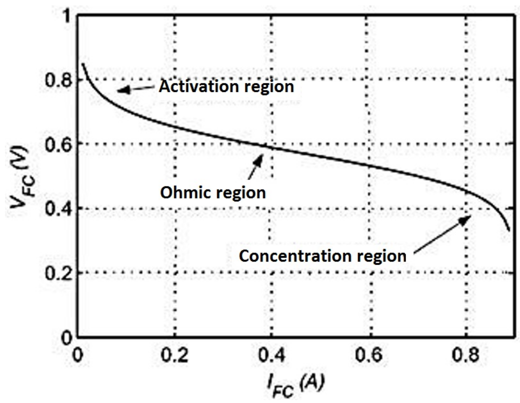

Figure 2. Voltage-Current characteristics of the fuel cell (Bucci *et al.*, 2006).

In order to obtain an experimental model to simulate the (output) behavior of a fuel cell as the current input varies one should detail the terms of equation (1) as follows. The thermodynamical equilibrium potential is given by the Nerst equation (Moreira and Silva, 2009):

$$E = E^0 + \frac{RT}{2F}\ln\left[P_{H_2}P_{O_2}^{\frac{1}{2}}\right] \qquad \text{with} \qquad E^0 = 1,229 - 0.85\times10^{-3}\left(T - 298,15\right)\,. \tag{2}$$

In additon, V_{act} can be expressed by (Revoredo, 2011):

$$V_{act} = \xi_1 + \xi_2 T + \xi_3 T\ln\left(C_{O_2}\right) + \xi_4 T\ln\left(i_{FC}\right), \tag{3}$$

where

$$C_{O_2} = \frac{P_{O_2}}{5,08\times10^6\times\exp\left(\frac{-498}{T}\right)}\,, \tag{4}$$

$$\xi_2 = 0,00286 + 0,0002\ln A_{FC} + 4,3\times10^{-5}\ln\left(C_{H_2}\right)\,, \tag{5}$$

$$C_{H_2} = \frac{P_{H_2}}{1,09\times10^6\times\exp\left(\frac{77}{T}\right)}\,. \tag{6}$$

The Ohmic loss can be determined by:

$$V_{ohmic} = i_{FC}\,(R_M + R_C) \tag{7}$$

with

$$R_M = \frac{\rho_M \times L}{A_{FC}} \qquad \text{and} \qquad \rho_M = \frac{181.6\left[1 + 0.03(\frac{i_{FC}}{A_{FC}}) + 0.062(\frac{T}{303})^2(\frac{i_{FC}}{A_{FC}})^{2.5}\right]}{[\psi - 0.634 - 3(\frac{i_{FC}}{A_{FC}})]\exp(4.18[\frac{T-303}{T}])}\,. \tag{8}$$

In the previous equation, the specific resistivity of the membrane is represented by $181/(\varphi - 0,634)$ considering $T = 303$K (30^oC) and $i_{FC} = 0$. The exponential term in the denominator is the temperature correction factor. The term between brackets in the numerator along with the term $3(i_{FC}/A_{FC})$ in the denominator are determined empirically (Revoredo, 2011), and represent the specific membrane resistivity correction as a function of the current density and the temperature of the fuel cell. The parameter ψ is adjustable depending on the membrane preparation and humidification, among other factors. The loss due to mass transport can be expressed by

$$V_{con} = -B \times \ln\left(1 - \frac{J_{FC}}{J_{max}}\right)\,, \tag{9}$$

where B (Volts) is a coefficient that depends on the cell parametrization and its operating point, while J_{FC} and J_{max} represent the actual and maximum current densities (A/cm^2), respectively. Typical values for J_{max} in a Proton Exchange Membrane Fuel Cell vary between 500 and 1500 mA/cm^2.

A PEMFC stack is formed by the series connection of n fuel cell (n integer). Thus, in order to find the output voltage and power of the fuel cell stack (V_s and P_s) one should simply multiply the unit cell voltage (V_{FC} and $P_{FC} := V_{FC}\times i_{FC}$) by the number of cells in the stack as follows:

$$V_s = n \times V_{FC} \qquad \text{and} \qquad P_s = n \times V_{FC} \times i_{FC}\,. \tag{10}$$

Conventionally, chemical energy is first converted into heat, which is then converted into mechanical energy, to finally be converted into electrical energy. However, in a fuel cell, chemical energy is directly converted into electrical energy. In an ideal scenario, the efficiency of a PEMFC would be given by the following equation:

$$\eta_{\text{ideal}} = \frac{\Delta G}{\Delta H} \tag{11}$$

with ΔG representing the change in the Gibbs free energy (in J/mol), and ΔH the variation of entropy (U.S. Department of Energy, 2000). For convenience, the efficiency of the fuel cell is often expressed in terms of the ratio of the operating voltage of the FC, V_{actual} and its ideal voltage E_{ideal}. Therefore, the thermal efficiency of FC can be calculated by:

$$\eta = \frac{\text{Usable Energy}}{\Delta H} = \frac{\text{Usable Power}}{\frac{\Delta G}{\eta_{\text{ideal}}}} = \frac{\eta_{\text{ideal}} \times V_{\text{actual}}}{E_{\text{ideal}}} \tag{12}$$

This efficiency discussion is important to show how the power generated (P_s) in (10) is dependent of the FC operation point, which is related to physical variables such as temperature, H_2 gas pressure, etc. In reference (O'Rourke *et al.*, 2009), it is shown that the relation between the variables P_s and i_{FC} is in general a nonlinear function with an extremum (maximum) point. Mathematically, we can express this it by:

$$P_s = h(i_{FC}) \tag{13}$$

with a global extremum point $P_s^* = h(i_{FC}^*)$. In Section 3. the function $h(\cdot)$ is approximated by a quadratic map $f(\cdot)$ so that the dither perturbation based ES can be directly applied with the input of the map being denoted by $\theta := i_{FC}$ and output $P_s = f(\theta)$. In Section 4. we use the straightforward notation $y := P_s$ and $x := i_{FC}$, without any kind of approximation for the nonlinear function $h(\cdot)$.

3. GRADIENT BASED EXTREMUM SEEKING

Many versions of extremum seeking exist, with various approaches to their stability study. The most common version employs perturbation signals for the purpose of estimating the gradient of the unknown map that is being optimized (Krstić, 2014). To understand the basic idea of extremum seeking, it is best to first consider the case of a static single-input map of the quadratic form, as shown in Figure 3.

Three different θ's appear in Figure 3: θ^* is the unknown optimizer of the map, $\hat{\theta}(t)$ is the real-time estimate of θ^*, and $\theta(t)$ is the actual input into the map. The actual input $\theta(t)$ is based on the estimate $\hat{\theta}(t)$ but is perturbed by the signal

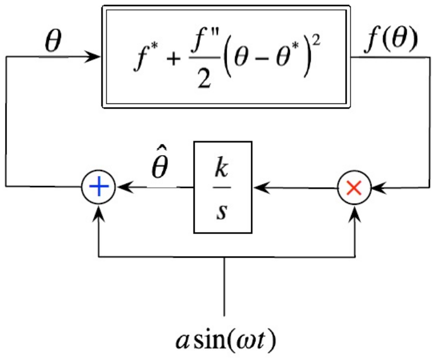

Figure 3. Figure extracted from (Krstić, 2014). The simplest perturbation-based extremum seeking scheme for a quadratic single-input map $f(\theta) = f^* + \frac{f''}{2}(\theta - \theta^*)^2$, where f^*, f'', θ^* are all unknown. The user has to only know the sign of $f''(< 0)$, namely, whether the quadratic map has a maximum, and has to choose the adaptation gain k such that $\mathrm{sgn}(k) = -\mathrm{sgn}(f'')$. The user has to also choose the frequency ω as relatively large compared to a, k, and f''.

$a\sin(\omega t)$ for the purpose of estimating the unknown gradient $f'' \cdot (\theta - \theta^*)$ of the map $f(\theta)$. The estimate $\hat{\theta}(t)$ is generated with the integrator k/s with the adaptation gain k controlling the speed of estimation.

The ES algorithm is successful if the error between the estimate $\hat{\theta}(t)$ and the unknown θ^*, namely the signal

$$\tilde{\theta}(t) := \hat{\theta}(t) - \theta^* \tag{14}$$

converges towards zero. Based on Figure 3, the estimate is governed by the differential equation $\dot{\hat{\theta}}(t) = k\sin(\omega t)f(\theta)$, which means that the estimation error is governed by

$$\frac{d\tilde{\theta}}{dt} = ka\sin(\omega t)\left[f^* + \frac{f''}{2}\left(\tilde{\theta} + a\sin(\omega t)\right)^2\right] . \tag{15}$$

By expanding the right-hand side one obtains

$$\frac{d\tilde{\theta}}{dt} = kaf^*\sin(\omega t) + ka^3\frac{f''}{2}\sin^3(\omega t) + ka\frac{f''}{2}\sin(\omega t)\tilde{\theta}(t)^2 + ka^2f''\sin^2(\omega t)\tilde{\theta}(t) . \tag{16}$$

A theoretically rigorous time-averaging procedure (Krstić, 2014) allows to replace the above sinusoidal signals by their means, yielding the "average system":

$$\frac{d\tilde{\theta}_{\mathrm{av}}}{dt} = \frac{kf''a^2}{2}\tilde{\theta}_{\mathrm{av}} , \tag{17}$$

which is exponentially stable since $kf'' < 0$. The averaging theory guarantees that there exists sufficiently large ω such that, if the initial estimate $\hat{\theta}(0)$ is sufficiently close to the unknown θ^*,

$$|\theta(t) - \theta^*| \leq |\theta(0) - \theta^*|\, e^{\frac{kf''a^2}{2}t} + \mathcal{O}(1/\omega) + a , \quad \forall t \geq 0 . \tag{18}$$

For the user, the inequality (18) guarantees that, if a is chosen small and ω is chosen large, the input $\theta(t)$ exponentially converges to a small interval around the unknown θ^* and, consequently, the output $f(\theta(t))$ converges to the vicinity of the optimal output f^*.

ES extends in a relatively straightforward manner from static maps to dynamic systems, provided the dynamics are stable and the algorithm's parameters are chosen so that the algorithm's dynamics are slower than those of the plant. The stability analysis in the presence of dynamics employs both averaging and singular perturbations, in a specific order. The design guidelines for the selection of the algorithm's parameters follow the analysis. Though the guidelines are too lengthy to state here, they ensure that the plant's dynamics are on a fast time scale, the perturbations are on a medium time scale, and the ES algorithm is on a slow time scale.

4. EXTREMUM SEEKING VIA MONITORING FUNCTION

We start summarizing some results obtained in (Aminde *et al.*, 2013) for relative degree one systems. The ES philosophy here is slightly different from the gradient approach presented in Section 3. Consider the simplest case of the integrator below with a nonlinear output mapping:

$$\dot{x} = u\,, \tag{19}$$
$$y = h(x)\,, \tag{20}$$

where $u \in \mathbb{R}$ is the control input, $x \in \mathbb{R}$ is the state vector and $y \in \mathbb{R}$ is the measured output of the static subsystem. The uncertain nonlinear function $h : \mathbb{R} \to \mathbb{R}$ to be maximized (or minimized) is locally Lipschitz continuous and sufficiently smooth. We assume that the initial time is $t = 0$ s. For each solution of (19)–(20) there exists a maximal time interval of definition given by $[0, t_M)$, where t_M may be finite or infinite.

4.1 Control Objective and Main Assumptions

The control objective of ES is not "stabilization" or "tracking", but is "real-time optimization" (Tan *et al.*, 2009). However, ES problem can be reformulated as a tracking problem in which the control direction is unknown (Aminde *et al.*, 2013). We wish to find an output-feedback control law u so that, from any initial condition, the system is steered to reach the extremum (maximum) point $y^* = h(x^*)$ of (20) and remain on such point thereafter, as close as possible.

By using the notation $h'(x) := \frac{\partial h(x)}{\partial x}$ and $h''(x) := \frac{\partial^2 h(x)}{\partial x^2}$, we consider that:

$(\mathbf{A1})$ (*On the objective function*): There exists a unique point $x^* \in \mathbb{R}$ such that $y^* = h(x^*)$ is the extremum (maximum) of $h(x)$: $\mathbb{R} \to \mathbb{R}$, satisfying

$$h'(x^*) = 0, \;\; h''(x^*) < 0$$
$$h(x^*) > h(x), \;\forall x \in \mathbb{R}, \; x \neq x^*$$

and for any given $\Delta > 0$, there exists a constant $L_h(\Delta) > 0$ such that

$$L_h(\Delta) \leq |h'(x)|, \forall x \notin \mathcal{D}_\Delta := \{x : |x - x^*| < \Delta/2\},$$

where $\mathcal{D}_\Delta$ is called Δ-vicinity of x^* and Δ can be made arbitrarily small by allowing a smaller L_h.

4.2 Basic Error Equation

From (19) and (20), the first time derivative of the output signal y is given by

$$\dot{y} = k_p(x)u\,, \tag{21}$$

where the high frequency gain (HFG), denoted by k_p, is the coefficient of u which appears in the first time derivative of the output y and it is given by

$$k_p(x) = h'(x)\,. \tag{22}$$

As in (Aminde *et al.*, 2013), the $\text{sgn}(k_p)$ is also called *control direction*. From (22) and $(\mathbf{A1})$, $k_p(x)$ satisfies

$$|k_p(x)| \geq \underline{k}_p > 0\,, \quad \forall x \notin \mathcal{D}_\Delta\,, \tag{23}$$

where $\underline{k}_p \leq L_h$ is a known constant lower bound for the HFG, considering all the admissible uncertainties in $h(\cdot)$.

The error signal e is given by

$$e(t) = y(t) - y_m(t)\,, \tag{24}$$

where $y_m \in \mathbb{R}$ is a simple ramp generated by the reference model

$$\dot{y}_m = r_m\,, \tag{25}$$

where $r_m > 0$ is a design constant. In order to avoid an unbounded reference signal $y_m(t)$ in the control scheme, one can saturate the model output at a rough known upper bound of y^* without affecting the control performance.

The key idea in (Aminde *et al.*, 2013) was to design a control law so that $y(t)$ tracks $y_m(t)$ as long as possible. In this way, y is forced to achieve the vicinity of the maximum $y^* = h(x^*)$ and remains close to the optimum value y^*. To this end, we have to propose u such that the output tracking error e tends to zero in finite time at least outside the Δ-vicinity, that is, in the neighborhood of the maximizer x^*.

Remark 1 It is straightforward to conclude that if $y = h(x)$ tries to track a increasing trajectory y_m, consequently, y must gradually approach the maximum at y^* as long as y remains away from a small vicinity of y^*, where the HFG is away from zero. Once y reaches the vicinity of y^*, the HFG will approach zero and thus observability is lost. Consequently, tracking of y_m will cease. But then, the neighborhood of the optimum point is already achieved as desired. The control strategy was developed to guarantee that y would remain close to y^* thereafter.

From (21), (24) and (25), by adding and subtracting $\lambda_m e$ to the time derivative of the error $e(t)$ one has

$$\dot{e} = k_p u - r_m + \lambda_m e - \lambda_m e \qquad \text{and} \qquad \dot{e} = -\lambda e + k_p(u + d_e)\,, \tag{26}$$

where $\lambda_m > 0$ is an arbitrary constant and

$$d_e := \frac{1}{k_p}[-r_m + \lambda_m e]\,. \tag{27}$$

4.3 Error Upper Bound

In (Aminde *et al.*, 2013), we have shown that if the control law

$$u = -\operatorname{sgn}(k_p)\rho\operatorname{sgn}(e) \tag{28}$$

was used with a nonnegative modulation function ρ satisfying

$$\rho \geq |d_e| + \delta\,, \tag{29}$$

and $\delta > 0$ being an arbitrarily small constant, then by using the Comparison Lemma (Filippov, 1964), one has $\forall t \in [t_i, t_M)$:

$$|e(t)| \leq \zeta(t)\,, \quad \zeta(t) := |e(t_i)|e^{-\lambda_m(t-t_i)}, \tag{30}$$

where $t_i \in [0, t_M)$.

The major problem is that $\operatorname{sgn}(k_p)$ is unknown, thus we could not implement it. In what follows, the switching scheme based on monitoring function is developed to cope with the lack of knowledge of the control direction outside the Δ-vicinity.

4.4 Monitoring Function based Control Law

In this case, the control law for plants with unknown HFG proposed by (Aminde *et al.*, 2013) is:

$$u = \begin{cases} u^+ &= -\rho(t)\operatorname{sgn}(e)\,, \quad t \in T^+\,, \\ u^- &= +\rho(t)\operatorname{sgn}(e)\,, \quad t \in T^-\,, \end{cases} \tag{31}$$

where the monitoring function is used to decide when u should be switched from u^+ to u^- and *vice versa*. In (31), $\rho(t) > 0$ is a continuous modulation function designed to satisfy (29 and the sets T^+ and T^- satisfy $T^+ \cap T^- = \emptyset$ and $T^+ \cup T^- = [0, t_M)$.

The detailed description of monitoring function can be found in (Oliveira *et al.*, 2010). Here, only a brief description of how it works is given. Reminding that inequality (30) holds when the control direction is correct, it seems natural to use ζ in (30) as a benchmark to decide whether a switching of u in (31) from u^+ to u^- (or u^- to u^+) is needed, *i.e.*, the switching occurs only when (30) is violated.

Therefore, consider the following function

$$\varphi_k(t) = |e(t_k)|e^{-\lambda(t-t_k)} + r, \tag{32}$$

where the t_k is the switching time and $r \geq 0$ is any arbitrarily small constant. The monitoring function φ_m is defined by

$$\varphi_m(t) := \varphi_k(t), \quad \forall t \in [t_k, t_{k+1}) \subset [0, t_M). \tag{33}$$

Note that from (32) and (33), one has $|e(t)| < |\varphi_k(t)|$ at $t = t_k$. Hence, t_k is defined as the time instant when the monitoring function $\varphi_m(t)$ meets $|e(t)|$, that is,

$$t_{k+1} := \begin{cases} \min\{t > t_k : |e(t)| = \varphi_k(t)\}, & \text{if it exists}\,, \\ t_M\,, & \text{otherwise}\,, \end{cases} \tag{34}$$

where $k \in \{1, 2, \ldots\}$ and $t_0 := 0\,\text{s}$.

By construction, the following inequality is directly obtained from (33)

$$|e(t)| \leq \varphi_m(t), \quad \forall t \in [0, t_M)\,. \tag{35}$$

A block diagram of the proposed monitoring function based ES controlling a fuel cell system is presented in Figure 4.

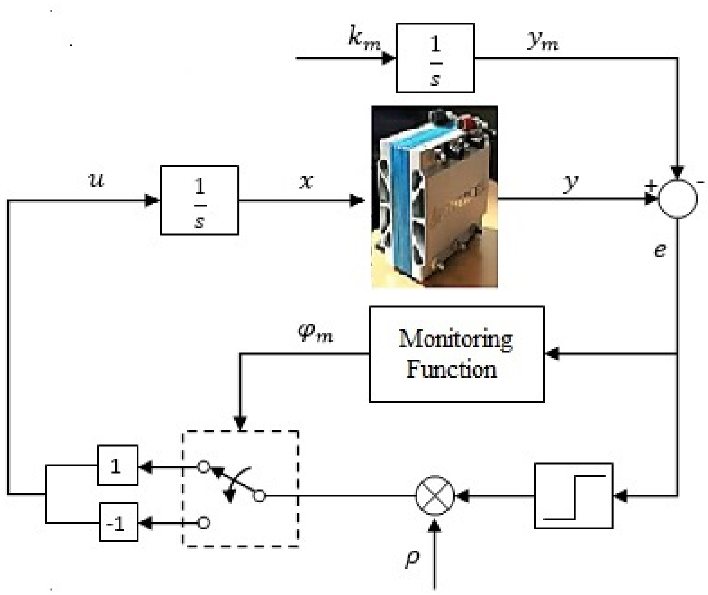

Figure 4. Block diagram of the proposed monitoring function based ES controlling a fuel cell system.

4.5 Stability Analysis

In the proposed scheme, the following proposition provides one possible modulation function implementation so that (29) holds and the control objectives can be attained.

Proposition 1 *Consider the system (19)–(20), the reference model (25) and control law (31). Outside of the Δ-vicinity $\mathcal{D}_\Delta$, if ρ in (31) is designed as*

$$\rho := \frac{1}{\underline{k}_p}\left[r_m + \lambda_m|e|\right] + \delta\,, \tag{36}$$

*then, while $x \notin \mathcal{D}_\Delta$, one has: **(a)** the monitoring function switching stops, **(b)** no finite-time escape of the system signals occurs, which implies that $t_M \to +\infty$, and **(c)** the error $y(t)$ tends to y^* in finite time. The term $\delta > 0$ is any arbitrary constant.*

Proof: The demonstration follows the same steps presented in the proof of (Aminde *et al.*, 2013, Proposition 1) since (19)–(20) is a particular case of relative degree one system. □

The following theorem states that the proposed output-feedback controller based on monitoring function drives x to the Δ-vicinity defined in **(A1)** of the unknown maximizer x^*. It does not imply that $x(t)$ remains in $\mathcal{D}_\Delta$, $\forall t$. However, the amplitude of signal oscillations around y^* can be kept of order $\mathcal{O}(r)$.

Theorem 1 *Consider the reference model (25) and the nonlinear system (19)–(20) with control law (31), modulation function (36) and monitoring function (32)–(33). Assume that **(A1)** holds, then: **(i)** the Δ-vicinity $\mathcal{D}_\Delta$ in **(A1)** is globally attractive being reached in finite time and **(ii)** for $L_h(r)$ in **(A1)** sufficiently small, the oscillations of $y(t)$ around the maximum value y^* can be made of order $\mathcal{O}(r)$, with r defined in (32). Since the signal y_m can be saturated in (25), all signals in closed-loop system remain uniformly bounded.*

4.6 Simulation Results

Due to the lack of space, we will omit a detailed description of the fuel-cell parameters used in our simulations. We simply invite the readers to consult reference (Revoredo, 2011) to check them. Although similar responses (curves not shown) can be obtained with the gradient ES method, faster convergence rates are obtained with the monitoring function approach introducted in Section 4. Figure 5 shows the excelent performance of the monitoring function based ES tracking the maximum power point under temperature variations.

5. REFERENCES

Aminde, N.O., Oliveira, T.R. and Hsu, L., 2013. “Global output-feedback extremum seeking control via monitoring functions”. *52nd IEEE Conference on Decision and Control*, pp. 1031–1036.

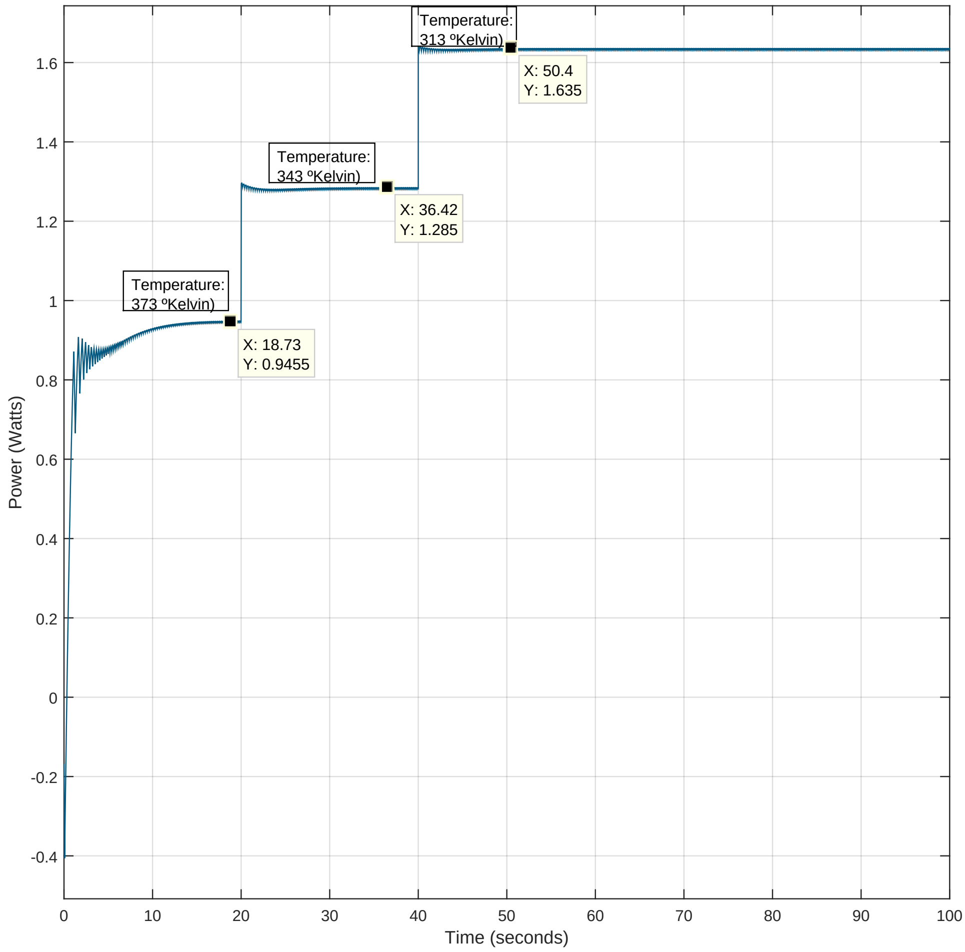

Figure 5. Variation of power versus time. The monitoring function algorithm shows uniform and fast transient with low steady-state error, even under temperature changes.

Bucci, G., Ciancetta, F., Fiorucci, E., Rotondale, E. and Veglio, F., 2006. "Experimental validation of a pem fuel cell dynamic model". *Proceedings of the International Symposium on Power Electronics, Electrical Drives, Automation and Motion*, Vol. 20, pp. 10–15.

CaSFCC, 2015. "California stationary fuel cell collaborative". *http://www.casfcc.org/*.

Filippov, A.L., 1964. "Differential equations with discontinuous right-hand side". *Amer. Soc. Translations*, Vol. 42, pp. 199–231.

Krstić, M., 2014. "Extremum seeking control". *in T. Samad and J. Baillieul, Encyclopedia of Systems and Control, Springer*.

Moreira, M.V. and Silva, G.E., 2009. "A practical model for evaluating the performance of proton exchange membrane fuel cells". *Renewable Energy*, Vol. 34, pp. 1734–1741.

Oliveira, T.R., Peixoto, A.J. and Hsu, L., 2010. "Sliding mode control of uncertain multivariable nonlinear systems with unknown control direction via switching and monitoring function". *IEEE Trans. Automat. Contr.*, Vol. 55, No. 4, pp. 1028–1034.

O'Rourke, J., Arcak, M. and Ramani, R., 2009. "Real-time optimization of net power in a fuel cell system". *Journal of Power Sources*, Vol. 187, pp. 422–430.

Revoredo, T.C., 2011. *Modelagem e gerenciamento de potência de um veículo elétrico híbrido de célula a combustível*. Master's thesis, COPPE/UFRJ.

Tan, Y., Nesić, D., Mareels, I.M.Y. and Astolfi, A., 2009. "On global extremum seeking in the presence of local extrema". *Automatica*, Vol. 45, pp. 245–251.

U.S. Department of Energy, Office of Fossil Energy, N.E.T.L., 2000. *Fuel cell handbook*. EG&G Services - Parsons, Inc. - Science Applications International Corporation, 5th edition.

Yau, H.T. and Wu, C.H., 2011. "Comparison of extremum-seeking control techniques for maximum power point tracking in photovoltaic systems". *Energies Jounal*, Vol. 4, pp. 2180–2195.